Hyperons, deconfinement, and the speed of sound in neutron stars

R. M. Aguirre

Departamento de Fisica, Facultad de Ciencias Exactas, Universidad Nacional de La Plata, and IFLP, UNLP-CONICET, C.C. 67 (1900) La Plata, Argentina

(Received 22 April 2022; accepted 13 June 2022; published 28 June 2022)

The effects on the speed of sound in neutron stars due to the presence of hyperons and a phase transition to deconfined quark matter is investigated. For this purpose a composite description within the covariant field theory is used; it consists of different models for the hadronic and for the unbound quark configurations. A phase transition with continuous and monotonous variation of the equation of state is assumed. The predictions obtained are contrasted with recent observational data on isolated neutron stars as well as on binary systems. Only one candidate is finally obtained from six different descriptions. According to the present calculations, the onset of the hyperons causes the equilibrium speed of sound to exceed the conformal limit. Based on recent works on the propagation of g-modes in neutron stars, different definitions of the speed of sound are considered.

DOI: 10.1103/PhysRevD.105.116023

I. INTRODUCTION

The study of the structure and dynamics of compact stars offers the possibility to test a unified theoretical description covering the many facets of the strong interaction in combination with gravitation. Therefore, it has been a subject of permanent interest, but in recent years it has concentrated multiplied efforts since an important amount of observational data has been acquired and analyzed.

The possibility to use different experimental techniques to focus on the same event or the same class of objects has created great expectations in the specialized community. This is particularly valid for the study of compact stars, as new and previous information have created a sketch of different aspects, such as the mass-radius relation, the cooling process, the emission of gravitational waves from binary mergers, etc. From the theoretical point of view it is expected that all this input will help to shed light on some longstanding puzzles and to improve the models and procedures used.

The evidence of very massive neutron stars with inertial masses above 2 $M_\odot$ [1–3] has introduced some tension with certain predictions of the relativistic field theory of hadrons. Calculations made in this framework, using a mean field approximation, have shown that the emergence of the hyperon population at densities well above the normal nuclear density produces an energetically favorable state. The persistence of the hyperons extends to extremely large densities and affects significatively the composition of the core of the star. However, most of these results do not admit a neutron star with mass as high as $M/M_\odot \simeq 2$. This situation is known in the literature as the hyperon puzzle. A similar picture is obtained when a deconfinement transition is considered. For this purpose a composite model is usually employed, corresponding to the hadronic phase and the deconfined quark-gluon plasma. A first-order transition, or even a coexistence of phases, lowers the energy of the system but also excludes the minimum upper bound for the star mass in most cases.

Closely related to the determination of the star masses is the mutual deformation of binary systems, due to gravitation as the mass distribution of the binary components becomes relevant at advanced stages of the inspiral process. In particular, the quotient of the quadrupole deformation to the perturbing tidal field is the only quantity characterizing its influence on the gravitational wave phase emitted in the early steps [4]. A partial answer to this problem was given by the first detection of a gravitational wave generated by the collapse of a binary system of neutron stars [5], from which the chirp mass of the system was determined with high precision to be $\mathcal{M}/M_\odot \simeq 1.19$. To obtain information about the masses of each component, two different regimes for the spin of the rotating stars are considered in [5]. Taking the adimensional parameter $j = cJ/GM^2$, where J is the total angular momentum, they find for $j < 0.89$ that $1.36 < m_1/M_\odot < 2.26$ and $0.86 < m_2/M_\odot < 1.36$. Whilst for $j < 0.05$ the results are $1.36 < m_1/M_\odot < 1.60$ and $1.16 < m_2/M_\odot < 1.37$. In addition the tidal deformability for a neutron star with mass 1.4 $M_\odot$ was bounded by $\Lambda_{1.4} \leq 800\,(970)$ for the case $j < 0.89\,(0.05)$. Further refinements [6] obtained the preferable values $1.36 < m_1/M_\odot < 1.62$, $1.15 < m_2/M_\odot < 1.36$, and $\Lambda_{1.4} = 190^{+390}_{.120}$.

The description of the neutron stars based on microscopic models of the strong interaction still suffers from important uncertainties. Intensive work has been devoted to contrast the recently obtained observational data with the predictions of a high variety of hadronic models [7–27].

Many of these studies have assumed that matter is composed of protons and neutrons as the only baryons. Hence the crucial requisite to accommodate neutron stars with mass at least of $M \simeq 2\, M_\odot$ is guaranteed [10]. However, in most cases, the mechanism which inhibits the onset of the hyperons is not explicitly stated. A smaller number of investigations include effects of the hyperons [11–17,20,24]. The possibility of a deconfinement phase transition including different types of realizations has been the subject of the thorough study [14] and also of [13,23]. For instance, the outcomes in [17] about the composition of the binaries in the GW170817 event depend on the amount of *a priori* information deposited on the sampling of equations of state. For the informed one the probability for a free quark phase is 56% against 44% for a pure hadronic phase. The less informed sample obtains a reversed 36% against 64%, respectively. The analysis made in [23], including data from GW170817 and GW190425 events, does not find evidence of a strong phase transition. Transitions including discontinuities in the thermodynamical potential have received special attention [8,20,21,24] because they present more evident effects, and also, they would be detectable by the postmerger gravitational wave [20].

An important feature of the equation of state (EOS) is the relativistic speed of sound v_s defined by $v_s^2 = c^2 dP/d\mathcal{E}$, where P and $\mathcal{E}$ are the pressure and the energy density of the system, respectively. The value $v_s/c = 1/\sqrt{3}$ has been considered as an upper bound based on very general arguments. The potential conflict between this assumption and the existence of massive neutron stars was pointed out in [28]. This observation has motivated several investigations on the role of an hypothetical upper limit of the speed of sound on the properties of neutron stars and binary systems [29–35]. It must be noted that [32] found that some equations of state, often considered as a paradigm, violates causality when the baryonic density takes large enough values. Much of these works go further with the approach used in [36], where the EOS is separated into a low density part described by a favorite model and a schematic high density contribution, depending on the speed of sound. The results obtained for the structure of neutron stars are then contrasted with the observational evidence, mainly the maximum mass and the tidal deformation of a pair of interacting stars. The possibility that matter is partially composed of hyperons at intermediate densities has not been considered in most of these references. However, [37] has paid special attention to this issue. Recently, these investigations have been extended by considering a nontrivial structure for the speed of sound in dense matter [38], including the effects of hyperons as well as different types of phase transitions. An interesting consequence of a deconfinement transition in the scenario of the inspiraling process of a binary system has been analyzed in [39]. If the principal mode of the nonradial gravitational oscillations (g-mode) and the tidal force are resonant, then this could affect the phase of the gravitational waveform. The frequency of these oscillations depends on the difference of the squared equilibrium and adiabatic speeds of sound. If the thermodynamical potentials are continuous through the transition, but the derivative $dP/d\mathcal{E}$ shows a finite discontinuity, then the same type of behavior is expected in the frequency of the g-mode. Thus, the speed of sound plays an important role in the description of an isolated neutron star as well as for a binary system. It is a direct measure of the stiffness of the EOS; it explicitly enters in the definition of the linearized metric perturbation, which is used in the evaluation of the second Love number, and determines the behavior of the frequency of the g-mode. For these reasons the aim of the present work is to analyze the speed(s) of sound under several circumstances.

This work is organized as follows: in the next section the general theoretical description is presented. Section III is devoted to describe the evaluation of some properties of a neutron star. Specific results are shown and discussed in Sec. IV, and finally, the conclusions are drawn in Sec. V. For the sake of completeness, some calculations on the quark effective masses are shown in the Appendix.

II. THEORETICAL DESCRIPTION

To describe the neutron star, several versions of the covariant field theory of hadrons are used. In these models the baryons couple linearly to mesons, and the latter exhibit different types of self-interactions. Thus the Lagrangian density can be written as

$$\begin{aligned}\mathcal{L}_H = &\sum_b \bar{\psi}_b (i\partial\!\!\!/ - M_b + g_{\sigma b}\sigma + g_{\xi b}\xi + g_{\delta b}\tau\cdot\delta - g_{\omega b}\omega\!\!\!/ - g_{\phi b}\phi\!\!\!/ - g_{\rho b}\tau\cdot\rho\!\!\!/)\psi_b \\ &+ \frac{1}{2}(\partial^\mu\sigma\partial_\mu\sigma - m_\sigma^2\sigma^2) - \frac{A}{3}\sigma^3 - \frac{B}{4}\sigma^4 + \frac{1}{2}(\partial^\mu\delta\cdot\partial_\mu\delta - m_\delta^2\delta^2) + G_{\sigma\delta}\sigma^2\delta^2 \\ &+ \frac{1}{2}(\partial^\mu\xi\partial_\mu\xi - m_\xi^2\xi^2) - \frac{1}{4}W^{\mu\nu}W_{\mu\nu} + \frac{1}{2}m_\omega^2\omega^2 + \frac{C}{4}\omega^4 - \frac{1}{4}R^{\mu\nu}\cdot R_{\mu\nu} \\ &+ \frac{1}{2}m_r^2\rho^2 + G_{\omega\rho}\rho^2\omega^2 - \frac{1}{4}F^{\mu\nu}F_{\mu\nu} + \frac{1}{2}m_\phi^2\phi^2, \end{aligned} \tag{1}$$

where the sum runs over the octet of baryons. In addition to the commonly used σ, ω, ρ mesons, here the scalar isovector field δ^a, with $a = 1-3$, as well as the hidden strangeness ξ, ϕ mesons, are also included. The δ and ξ particles can be identified with the a_0 (980) and $f_0(980)$ states, respectively. The ξ, ϕ are assumed as mainly composed by a $s\bar{s}$ pair, and therefore, they couple only to the hyperons. The coupling constants $g_{mb}, m = \sigma, \xi, \delta, \omega, \rho, \phi$ and $A, B, C, G_{\sigma\delta}, G_{\sigma\delta}$ vary from one model to another and are fixed to reproduce different sets of empirical data. The equations of motion corresponding to this Lagrangian are solved in the mean field approximation for uniform dense matter, in a reference frame where the mean value of the spatial component of the baryon currents are zero. Furthermore, all the degrees of freedom are considered as stable states of the strong interaction. Under such conditions the equations are greatly simplified since the meson mean values do not vary spatially, and only the third component of the isomultiplets are nonzero,

$$
\begin{aligned}
&(i\partial\!\!\!/ - M_b^* - g_{\omega b}\omega_0 - g_{\phi b}\phi_0 - g_{\rho b} I_b \rho_0)\psi_b = 0,\\
&(m_\sigma^2 - 2G_{\sigma\delta}\delta^2)\sigma + A\sigma^2 + B\sigma^3 = \sum_b g_{\sigma b} n_{sb},\\
&(m_\delta^2 - 2G_{\sigma\delta}\sigma^2)\delta = \sum_b g_{\delta b} n_{sb},\\
&m_\xi^2 \xi = \sum_b g_{\xi b} n_{sb},\\
&(m_\omega^2 + C\omega_0^2 + 2G_{\omega\rho}\rho_0^2)\omega_0 = \sum_b g_{\omega b} n_b,\\
&(m_\rho^2 + 2G_{\omega\rho}\omega_0^2)\rho_0 = \sum_b g_{\rho b} I_b n_b,\\
&m_\phi^2 \phi_0 = \sum_b g_{\phi b} n_b,
\end{aligned}
$$

where I_b is the 3 isospin component, $M_b^* = M_b - g_{\sigma b}\sigma - g_{\xi b}\xi - g_{\delta b} I_b \delta$ is the effective mass of the baryon b, and the source of the meson equations are the baryon densities

$$
n_b = \frac{p_b^3}{3\pi^2}, \qquad n_{sb} = \frac{M_b^*}{2\pi^2}\left[p_b E_b - M_b^{*2} \ln\left(\frac{p_b + E_b}{M_b^*}\right)\right].
$$

The left side equation introduces the Fermi momentum, and $E_b = \sqrt{p_b^2 + M_b^{*2}}$ is used. Within the approach, the energy density of the system is given by

$$
\begin{aligned}
\mathcal{E}_H = &\frac{1}{4}\sum_b (n_{sb} M_b^* + 3 n_b E_b)\\
&+ \frac{1}{2}(m_\sigma^2\sigma^2 + m_\delta^2\delta^2 + m_\xi^2\xi^2 + m_\omega^2\omega_0^2 + m_\rho^2\rho_0^2 + m_\phi^2\phi^2)\\
&+ \frac{A}{3}\sigma^3 + \frac{B}{4}\sigma^4 - G_{\sigma\delta}\sigma^2\delta^2 + \frac{3}{4}\omega_0^2(C\omega_0^2 + 4G_{\omega\rho}\rho^2).
\end{aligned}
$$

The pressure is obtained by the canonical relation

$$
P = \sum_b \mu_b n_b - \mathcal{E}_H,
$$

and the chemical potentials are given by $\mu_b = E_b + g_{\omega b}\omega_0 + g_{\phi b}\phi_0 + g_{\rho b} I_b \rho_0$.

Three specific versions of the general expression (1) are used in this work. The first one is based on the GM1 model of [40], which takes as reference values $n_0 = 0.153$ fm^{-3} for the normal nuclear density, and $E_{\rm bind} = -16.3$ MeV, $E_{\rm sym} = 32.5$ MeV, $M_N^*/M_N = 0.7$, and $K = 300$ MeV for the binding energy, the symmetry energy, the effective nucleon mass, and the nuclear compressibility in normal conditions. These constraints determine the constants $g_{\sigma N}, g_{\omega N}, g_{\rho N}, A$, and B which can be consulted in [40]. The model has been updated in [41] by introducing the couplings between hyperon and vector mesons according to the SU(6) symmetry of the quark model

$$
\begin{aligned}
&g_{\omega\Lambda} = g_{\omega\Sigma} = 2g_{\omega\Xi} = \frac{2}{3} g_{\omega N}; \quad g_{\rho\Lambda} = 0,\\
&\frac{1}{2} g_{\rho\Sigma} = g_{\rho\Xi} = g_{\rho N};\\
&g_{\phi\Lambda} = g_{\phi\Sigma} = \frac{1}{2} g_{\phi\Sigma} = -\frac{\sqrt{2}}{3} g_{\phi N}.
\end{aligned}
$$

The scalar mesons ξ, δ are discarded in this scheme, and all the constants $C, G_{\sigma\delta}, G_{\omega\rho}$ are taken as zero. The remaining three parameters $g_{\sigma b}, b = \Lambda, \Sigma, \Xi$ are determined by adjusting the energy $U_b = g_{\omega b}\omega - g_{\sigma b}\sigma$ (subtracting the vacuum rest mass) of an isolated hyperon at rest, immersed in isospin symmetric nuclear matter at the normal density. Although their empirical values are not well known, they are usually taken as

$$
U_\Lambda = -30 \text{ MeV}, \qquad U_\Sigma = 30 \text{ MeV}, \qquad U_\Xi = -18 \text{ MeV}. \tag{2}
$$

Motivated by the uncertainty just mentioned, Ref. [41] analyzed the effect of the variation of $U_b, b = \Sigma, \Xi$ on the maximum mass $M_{\rm max}$ of an isolated neutron star. It was found that keeping U_Ξ fixed and varying $-40 < U_\Sigma[\text{MeV}] < 40$ produce small changes and always $M_{\rm max} < 2\ M_\odot$. Inversely, if U_Σ is kept fixed, it is found that the maximum mass increases monotonously with U_Ξ, reaching $M_{\rm max} = 2.04\ M_\odot$ for $U_\Xi = 40$ MeV. Therefore, the more optimistic case with $U_\Xi = 40$ MeV is adopted in this work, obtaining the following values $g_{\sigma\Lambda}/g_{\sigma N} = 0.617$, $g_{\sigma\Sigma}/g_{\sigma N} = 0.404$, and $g_{\sigma\Xi}/g_{\sigma N} = 0.113$. The parametrization thus obtained will be labeled as GM1e. The second model is based on the NL3 parametrization [42], which was adjusted to describe with acceptable accuracy the properties of several atomic nuclei. It gives the following

results for uniform isospin symmetric nuclear matter $n_0 = 0.148\,\mathrm{fm}^{-3}$, $E_{\mathrm{bind}} = -16.3$ MeV, $E_{\mathrm{sym}} = 37.4$ MeV, $M_N^*/M_N = 0.6$, and $K = 271.7$ MeV. The original version was taken further in [43], introducing hyperons in interaction through the scalar and vector mesons ξ and ϕ, respectively. As in the previous case the hyperon-vector meson couplings are related to $g_{\omega N}, g_{\rho N}$ by assuming SU(6) symmetry, and the scalar sector is adjusted to satisfy the constraints (2). It must be noted that $g_{\xi b}$ does not participate in these relations since they are defined at zero hyperon density, hence there is some freedom for choosing these couplings. We adopt here the set labeled as "weak YY" in [43], so the numerical values of the parameters are taken from this reference. To complete the comparison with Eq. (1) it must be said that the δ meson is not considered, hence $G_{\sigma\delta} = 0$ and also $C = G_{\omega\rho} = 0$. This prescription will be denoted as NL3e in the following.

Finally, the third model (M$\sigma\delta$) has recently been proposed [44] with the aim of study on how the properties of the neutron stars are affected by mixing interactions between the $\sigma - \delta$ scalar mesons. The prescription of [45] is adopted to choose the model parameters. Thus the reference empirical values $n_0 = 0.16\ \mathrm{fm}^{-3}$, $E_{\mathrm{bind}} = -16$ MeV, $E_{\mathrm{sym}} = 32$ MeV, $M_N^*/M_N = 0.65$, and $K = 230$ MeV are taken, and the slope parameter of the symmetry energy $L = 50$ MeV is reproduced in addition. In the present work this formulation is complemented with the inclusion of hyperons and the ϕ vector meson. In order to simplify the scheme, the scalar meson ξ is not considered here, and the coupling of the δ meson to the hyperons is taken as zero. Eventually, the last items will be the subject of future work. The hyperon-vector mesons are fixed according the SU(6) symmetry scheme, and the hyperon-scalar meson couplings follow from (2), obtaining in this way $g_{\sigma\Lambda} = 5.616$, $g_{\sigma\Sigma} = 3.989$, and $g_{\sigma\Xi} = 2.920$.

The hypothesis of homogeneous matter, which lead to the equations of motion shown above, is appropriate for a range of densities above several tenths of the normal nuclear value n_0. The electromagnetic interaction, not included in (1), gives rise to nonhomogeneous structures. For this reason the equation of state evaluated in [46] is adopted for the low density regime and assembled to the results of the interaction (1) by imposing continuity at the joining point. At the other extreme, for very dense matter it is expected that hadrons are no longer the most stable configuration of bound quarks and a transition to deconfined quarks happens. To take account of a state of homogeneous quark matter, two different descriptions are examined in this work, the Nambu Jona-Lasinio (NJL) and the bag (BM) models. In the schematic BM the noninteracting quarks have a current mass and a change of scale due to nonperturbative effects are represented by the bag constant B added to the thermodynamical potential. The NJL, instead, presents interacting quarks which generate their own constituent masses. This effective mass depends on the properties of the medium and are expected to decrease with increasing baryonic density. The energy density for both models are as follows:

$$\begin{aligned}\mathcal{E}_{\mathrm{Q}}^{\mathrm{BM}} &= \frac{N_c}{\pi^2}\sum_q \int_0^{p_q} dp\, p^2\sqrt{p^2+m_q^2} + B,\\ \mathcal{E}_{\mathrm{Q}}^{\mathrm{NJL}} &= \frac{N_c}{\pi^2}\sum_q \left[\int_\Lambda^{p_q} dp\, p^2\sqrt{p^2+M_q^2} + 2Gn_{sq}\right]\\ &\quad - 4Kn_{su}\,n_{sd}\,n_{ss} + \mathcal{E}_0, \end{aligned} \tag{3}$$

where $q = u, d, s$, p_q is the Fermi momentum, which is related to the baryonic number density by $n_q = p_q^3/3\pi^2$, and m_q is the current quark mass. The total baryon number density is represented by $n_{\mathrm{Q}} = \sum_q n_q$. In particular, the NJL model uses a cutoff Λ for the momentum integration, G and K are the couplings for four and six quark interactions, $\mathcal{E}_0$ is a constant introduced to obtain zero vacuum energy, and the effective masses are given by

$$M_i = m_i - 4Gn_{si} + 2Kn_{sj}n_{sk}, \qquad j \neq i \neq k.$$

The quark condensates n_{sq} can be expressed as

$$n_{sq} = \frac{N_c}{\pi^2} M_q \int_\Lambda^{p_q} \frac{dp\, p^2}{\sqrt{p^2+M_q^2}}.$$

The chemical potential for each flavor is simply $\mu_q = \sqrt{p_q^2+m_q^2}$ within the BM, or $\mu_q = \sqrt{p_q^2+M_q^2}$ in the NJL.

The transition between the hadronic and deconfined phases has been described in different dynamical schemes. In this work the picture of a continuous and monotonous equation of state, with an intermediate state of coexisting phases is adopted. It is commonly denominated as the Gibbs construction. If χ is the spatial fraction occupied by the deconfined phase, then the total energy and the baryonic number densities of the system are given by

$$\mathcal{E} = \chi\mathcal{E}_{\mathrm{Q}} + (1-\chi)\mathcal{E}_{\mathrm{H}}, \tag{4}$$

$$n = \chi n_{\mathrm{Q}} + (1-\chi)n_{\mathrm{H}}. \tag{5}$$

Furthermore, for thermodynamical equilibrium of the coexisting phases the partial pressures of each phase must coincide,

$$P_B = \sum_b \mu_b\, n_b - \mathcal{E}_{\mathrm{H}} = \sum_q \mu_q\, n_q - \mathcal{E}_{\mathrm{Q}}. \tag{6}$$

To describe neutron star matter the complementary requirement of electrical neutrality is imposed. To reach this condition a fluid of noninteracting leptons (electrons

and muons) is considered, which freely distributes among the hadron and quark phases so that the condition

$$0 = 3\chi\sum_q C_q n_q + (1-\chi)\sum_b C_b n_b - \sum_l n_l \qquad (7)$$

is satisfied. In this expression C_k stands for the electric charge in units of the positron charge. These leptons also contribute to the total energy by

$$\mathcal{E}_{\rm L} = \frac{1}{\pi^2}\sum_l \int_0^{p_l} dp\, p^2\sqrt{p^2+m_l^2},$$

where $n_l = p_l^3/3\pi^2$; their chemical potentials can be written as $\mu_l = \sqrt{p_l^2+m_l^2}$, and the partial lepton contribution to the pressure is $P_L = \sum_l \mu_l n_l - \mathcal{E}_{\rm L}$. Hence, the complete expressions for the energy and the pressure in the mixed phase are

$$\mathcal{E} = \chi\mathcal{E}_{\rm Q} + (1-\chi)\mathcal{E}_{\rm H} + \mathcal{E}_{\rm L}, \qquad (8)$$

$$P = \mu_{\rm B} n - \mathcal{E} = P_{\rm B} + P_{\rm L}. \qquad (9)$$

The coefficient χ is obtained by using the conditions of conservation of the baryonic number, the electric charge, and thermodynamical equilibrium, Eqs. (5), (7), and (6), respectively. Thus, it is uniquely determined for each density of neutral matter in equilibrium at zero temperature, and it is a dynamical property of the combination of models used.

There are two conserved charges which characterize the global state of the system, the baryonic number and the electric charge with associated chemical potentials $\mu_{\rm B}$ and $\mu_{\rm C}$, respectively. It must be noted that the last one does not enter in the intermediate expression of Eq. (9) because the total electric charge is zero. Both chemical potentials can be combined to give the chemical potentials of all baryons, quarks, and leptons circumstantially present. Therefore, they are linearly dependent through the relations of equilibrium against beta decay.

III. PROPERTIES OF THE NEUTRON STAR

The EOS is the main input to determine the structure of a neutron star. In our approach the relation between P and $\mathcal{E}$ is monotonous and continuous. However, its first derivative, i.e., the speed of sound, presents finite discontinuities at the threshold of the phase transition. Due to the bijectivity of the relation $P(\mathcal{E})$ one can write

$$c_s^2 = \frac{dP}{d\mathcal{E}} = \frac{dP/dn}{d\mathcal{E}/dn}.$$

Using Eqs. (5), (6), and (8) it can be shown that in the mixed phase is $d\mathcal{E}/dn = \mu_{\rm B}$, so that $dP/dn = nd\mu_{\rm B}/dn$, and finally

$$c_s^2 = \frac{n}{\mu_{\rm B}}\frac{d\mu_{\rm B}}{dn}. \qquad (10)$$

Although the expression (10) is quite simple, the evaluation could be difficult due to the large number of degrees of freedom and the constraints imposed. For pure hadronic matter, the derivative in Eq. (10) depends on the number N of baryonic species present in the Fermi sea,

$$\frac{d\mu_{\rm B}}{dn} = \frac{\det U}{\det V}. \qquad (11)$$

Here U, V are square matrices of $N+1$ columns with elements

$$\begin{aligned} U_{iN+1} &= \delta_{i,N+1}; \quad V_{iN+1} = 1-\delta_{i,N+1},\\ U_{N+1j} &= V_{N+1j} = (p_j/\pi)^2, \quad 1 \le j \le N,\\ U_{ij} &= -V_{ij} = H_{ij}, \quad 1 \le i,j \le N, \end{aligned}$$

where

$$\begin{aligned} H_{ij} = \left(\frac{p_j}{\pi}\right)^2 \Bigg\{ & -\frac{M_i^*}{E_i}\frac{M_j^*}{E_j}\frac{1}{\Delta}(\alpha_1 g_{\sigma i}g_{\sigma j} + \alpha_2 g_{\nu i}g_{\nu j} - \beta g_{\sigma i}g_{\nu j} - \beta g_{\sigma j}g_{\nu i})\\ & + \frac{1}{\Delta_V}[(m_\rho^2 + 2G_{\omega\rho}\omega_0^2)g_{\omega i}g_{\omega j} + (m_\omega^2 + 3C\omega_0^2 + 2G_{\omega\rho}\rho_0^2)g_{\rho i}g_{\rho j} - 4G_{\omega\rho}\omega\rho(g_{\omega i}g_{\rho j} + g_{\omega j}g_{\rho i})]\\ & + \frac{g_{\phi i}g_{\phi j}}{m_\phi^2} + \frac{\pi^2 C_i C_j}{\sum_l \mu_l p_l}\Bigg\} + \frac{p_j}{E_j}\delta_{i,j}, \end{aligned}$$

$$\alpha_1 = m_\sigma^2 - 2G_{\sigma\delta}\delta^2 + 2A\sigma + 3B\sigma^2 + \sum_b g_{\sigma b}^2\lambda_b, \qquad \alpha_2 = m_\nu^2 - 2G_{\sigma\delta}\sigma^2 + \sum_b g_{\nu b}^2\lambda_b,$$

$$\beta = \frac{1}{\pi^2}\sum_b g_{\sigma b}g_{\nu b}\lambda_b - 4G_{\sigma\delta}\sigma\delta, \qquad \lambda_b = \frac{1}{\pi^2}\int_0^{p_b}\frac{dp\, p^4}{(p^2 + M_b^{*2})^{3/2}},$$

$$\Delta_V = (m_\omega^2 + 2G_{\omega\rho}\rho_0^2 + 3C\omega_0^2)(m_\rho^2 + 2G_{\omega\rho}\omega_0^2) - (4G_{\omega\rho}\omega_0\rho_0)^2,$$

and $\Delta = \alpha_1\alpha_2 - \beta^2$. The scalar sector of the last expressions must be adapted to the model used; for the GM1e and NL3e cases one must take $\nu = \xi$, and $\nu = \delta$ for the M$\sigma\delta$ one.

The structure of Eq. (11) also holds in the coexistence phase, but in this case is

$$\begin{aligned}
U_{iN+1} &= S\delta_{i,N+1}, \quad 1 \le 1 \le N+1,\\
V_{N+1N+1} &= \frac{1}{S}\left\{\chi N_c\sum_q\left[\frac{S + 3C_q(n_{\rm H} - n_{\rm Q})}{3\pi}\right]^2 + \left(\frac{n_{\rm H} - n_{\rm Q}}{\pi}\right)^2\sum_l \mu_l p_l\right\},\\
V_{iN+1} &= C_i\frac{n_{\rm Q} - n_{\rm H}}{S} - 1, \quad 1 \le i \le N,\\
U_{N+1j} &= V_{N+1j} = (1-\chi)[S + C_j(n_{\rm H} - n_{\rm Q})]\left(\frac{p_j}{\pi}\right)^2, \quad 1 \le j \le N,\\
U_{ij} &= V_{ij} = H_{ij} - \frac{C_i C_j p_j^2}{\sum_l \mu_l p_l}, \quad 1 \le i, j \le N,
\end{aligned}$$

where $S = \sum_q n_q C_q - \sum_b n_b C_b$ has been used.

Finally, in pure quark matter it is found

$$\frac{d\mu_{\rm B}^0}{dn} = 3\pi^2\frac{3\sum_q \mu_q p_q C_q^2 + \sum_l \mu_l p_l}{N_c\mu_u\mu_d p_u(p_d + p_s) + \sum_q \mu_q p_q \sum_l \mu_l p_l}$$

within the BM. Whereas in the NJL the more intricate expression

$$\begin{aligned}
\frac{d\mu_{\rm B}}{dn} = \frac{d\mu_{\rm B}^0}{dn} &+ M_u'\frac{M_u}{\mu_u} + 2M_d'\frac{M_d}{\mu_d} + \frac{3}{\mu_u\mu_d}\\
&\times\frac{p_s(M_dM_d' - M_sM_s')\sum_q p_q\mu_q C_q + (2p_u\mu_u + \sum_l p_l\mu_l)(M_u'\frac{M_u}{\mu_u} + 2M_d'\frac{M_d}{\mu_d})\sum_l p_l\mu_l}{N_c\mu_u\mu_d p_u(p_d + p_s) + \sum_q \mu_q p_q\sum_l \mu_l p_l}
\end{aligned}$$

is obtained due to the variation of the constituent quark masses. Explicit formulas for these quantities are given in the Appendix.

The adiabatic speed of sound $\nu_a = \partial\mu_B/\partial n$ enters in the evaluation of the frequency of nonradial oscillations in compact stars [39]. It is obtained by imposing the condition that the relative population of each fermion species remains constant, even if β equilibrium is not verified. All the physical constraints are imposed after evaluation of the derivatives.

In pure hadronic matter the following result holds:

$$\begin{aligned}
v_a^{\rm H} = \frac{1}{n\mu_{\rm B}}\Bigg\{&\sum_b \frac{p_b^2}{3}\frac{n_b}{E_b} + \sum_l \frac{p_l^2}{3}\frac{n_l}{\mu_l} - \frac{1}{\Delta}(\alpha_1 X_\sigma^2 + \alpha_2 X_\nu^2 - 2\nu X_\nu X_\sigma) + m_\phi^2 X_\phi^2\\
&+ \frac{1}{\Delta_V}[(m_\rho^2 + 2G_{\omega\rho}\omega_0^2)X_\omega^2 + (m_\omega^2 + 3C\omega_0^2 + 2G_{\omega\rho}\rho_0^2)X_\rho^2 - 8G_{\omega\rho}X_\omega X_\rho]\Bigg\},
\end{aligned}$$

where

$$X_\alpha = \sum_b g_{\alpha b}\, n_b\frac{M_b^*}{E_b} \quad \text{for } \alpha = \sigma, \delta, \xi; \quad X_\alpha = \sum_b g_{\alpha b} n_b \quad \text{for } \alpha = \omega, \rho, \phi.$$

The treatment of pure quark matter gives, instead,

$$v_a^{\mathrm{Q}} = \frac{1}{3n\mu_{\mathrm{B}}}\left(\sum_q p_q^2 \frac{n_q}{\mu_q} + \sum_l p_l^2 \frac{n_l}{\mu_l}\right)$$

within the BM, and

$$v_a^{\mathrm{Q}} = \frac{1}{3n\mu_{\mathrm{B}}}\left(\sum_q p_q^2 \frac{n_q}{\mu_q} + \sum_l p_l^2 \frac{n_l}{\mu_l}\right) + \frac{1}{\mu_{\mathrm{B}}}\sum_q n_q M_q' \frac{M_q}{\mu_q}$$

for the NJL. In the domain of coexistence of phases one can write $v_a = \chi v_a^{\mathrm{Q}} + (1-\chi) v_a^{\mathrm{H}}$.

The structure of an isolated neutron star can be solved using the Tolman-Oppenheimer-Volkov equations for the spherically symmetric case

$$\frac{dP}{dr} = -(G/c^2)\frac{[\mathcal{E}(r)+P(r)][m(r)+4\pi r^3 P(r)/c^2]}{r^2[1-2(G/c^2)m(r)/r]},$$

$$\mathcal{M}(r) = \int_0^r 4\pi r'^2 [\mathcal{E}(r')/c^2] dr'.$$

Starting from given values of the central pressure and energy, these equations are integrated outward until a radius R is reached for which $P(R) = 0$, and the total mass is defined as $M = \mathcal{M}(R)$. Once the mass $\mathcal{M}(r)$ and pressure $P(r)$ distributions inside the star have been determined one can evaluate the second Love number k_2. For this purpose the radial function $y(r)$, related to the tidal field, must be found by solving the differential equation

$$y'(r) + y^2(r) + f(r)y(r) + q(r)r^2 = 0,$$

subject to the condition $y(0) = 2$. The following definitions have been used:

$$f(r) = \frac{1 + 4\pi r^2(P-\mathcal{E})}{1-2\mathcal{M}/r},$$

$$q(r) = \left[4\pi\left(5\mathcal{E} + 9P + \frac{P+\mathcal{E}}{v_s^2}\right) - \frac{6}{r^2} - \frac{4}{r^4}\frac{(\mathcal{M}+4\pi r^3 P)^2}{1-2\mathcal{M}/r}\right]/(1-2\mathcal{M}/r).$$

Then, the Love number is given by

$$k_2 = \frac{8}{5}x^5(1-2x)^2[2-y_R+2x(y_r-1)]/\{6x[2-y_R+x(5y_R-8)] + 4x^3[13-11y_R+x(3y_R-2) + 2x^2(1+y_R)] + 3(1-2x)^2[2-y_R+2x(y_R-1)]\ln(1-2x)\},$$

where $x = M/GR$ and $y_R = y(R)$. The tidal deformability is obtained in this approach as $\Lambda = 2k_2/3x^5$.

IV. RESULTS AND DISCUSSION

In this section a comparative analysis of the results provided by the different models is made. In first place I focus on the evidence that can be found in the speed of sound propagating in a neutron star, about the emergence of exotic degrees of freedom. Furthermore, an analysis is presented on the ability of the proposed framework to accommodate the observational evidence about compact stars.

Numerical evaluation of the hadronic properties has been done by using the parameter sets discussed in Sec. II. For the quark sector I use either the BM with parameters $B = 200$ MeV/fm^3, $m_u = m_d = 5$ MeV, and $m_s = 150$ MeV or the NJL model with the SU(3) parametrization given in [47].

Since there are many works that disregard the role of the hyperons in high density matter and with the purpose of contrast with this standard approach, for each of the hadronic models previously described I consider the case with hyperons artificially suppressed (NH).

The EOS obtained in different schemes is shown in Fig. 1. In each panel a low energy regime can be distinguished where all the curves coalesce. It is composed by pure nuclear matter and leptons. In the high energy extreme, instead, two different curves indicate the emergence of the pure quark phase as described by the BM or the NJL models. In general, the BM reaches this instance with lower pressures but steeper slope, i.e., with higher speed of sound. Between these extremes and as the energy increases, the emergence of the Λ hyperon and of deconfined quarks takes place, in the mentioned order. For the NL3e and M$\sigma\delta$ the heavier Ξ^- is also present, but in every case no new hyperon species appear during the coexistence. On the contrary, in the M$\sigma\delta$ description the preexistent Ξ^-

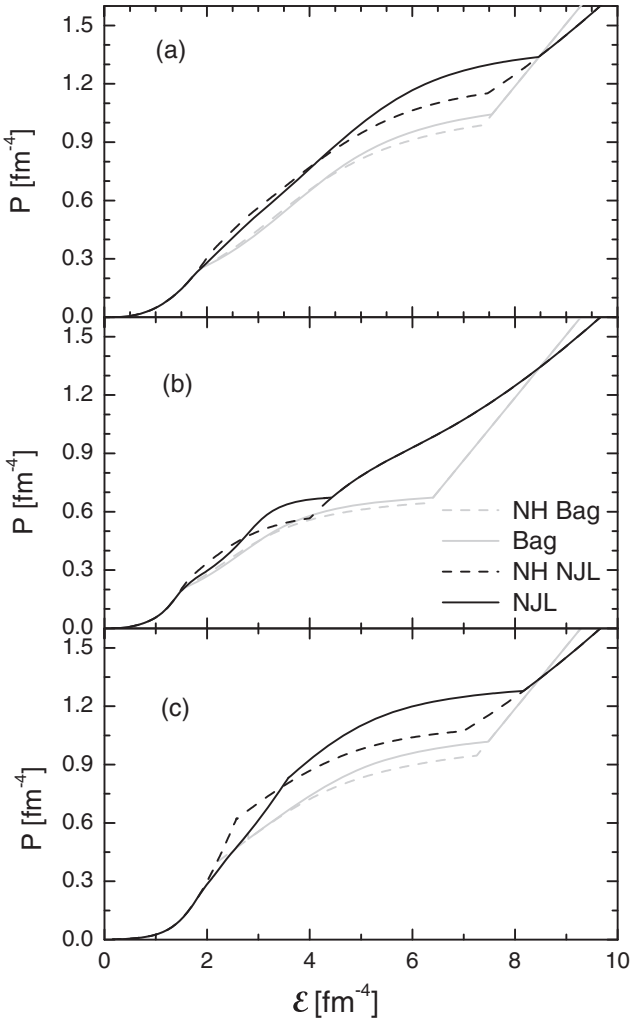

FIG. 1. The equation of state for the hadronic models GM1e (a), NL3e (b), and M$\sigma\delta$ (c). The cases with or without hyperons (NH) have been distinguished according to the line convention shown.

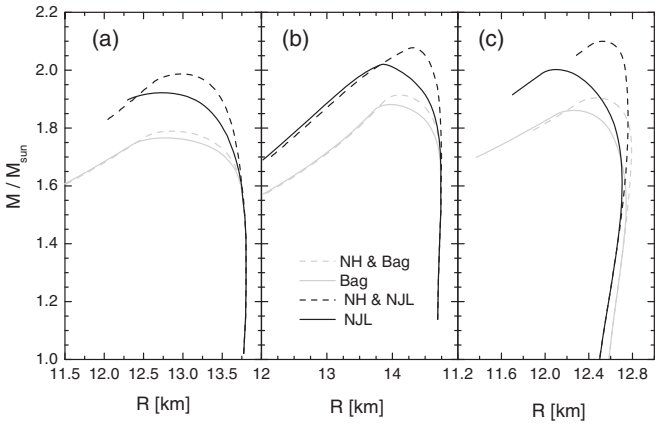

FIG. 2. The mass-radius relation for an isolated neutron for the hadronic models GM1e (a), NL3e (b), and M$\sigma\delta$ (c). The cases with or without hyperons (NH) have been distinguished according to the line convention shown.

population extinguishes before the phase transition is completed. It is evident that for all the hadronic models the combination with the BM produces an EOS softer than that corresponding to the NJL. The only exception is found for pure quark matter at extremely high energies, corresponding to densities above 2.5×10^{15} g/cm^3. Comparing results with or without hyperons, a common pattern is found; for lower values of $\mathcal{E}$ the pressure is slightly higher for the NH case, but beyond a particular value the relation is inverted. The point where this change happens is located in the coexistence phase. The enhancement of the pressure for relatively high energy, in the case of matter containing hyperons, is particularly noticeable when the NJL model is used. This feature deserves special emphasis because it corresponds to a regime accessible to the core of massive neutron stars. A contrast of the different models shows that in the NL3e the deconfinement starts at a lower pressure and has a stronger softening effect on the EOS. Furthermore, the coexistence region is wider for the BM than for the NJL model, thus pure quark matter appears earlier in the last case. Using this model I have verified that the threshold for the transition increases with the value chosen for the parameter B of the bag model. Thus in order to obtain stable pure hadronic matter for densities below 5×10^{14} g/cm^3 (around twice normal nuclear density) the bound $B \geq 200$ MeV/fm^3 must be satisfied. To give a uniform treatment, the same value $B = 200$ MeV/fm^3 is used in combination with all the hadronic descriptions. In regard to the remaining models, the critical pressure is lower for the GM1e than for the M$\sigma\delta$, and the slope of the EOS is higher in the last case. Therefore, it is expected that the transition to the outer crust of the neutron star develops more rapidly in the M$\sigma\delta$ model. The pressure at the density $n/n_0 = 2$ has been estimated in [6] as $P = 3.5^{+2.7}_{-1.7}$ dyn/cm^2 in order to be consistent with the observational data obtained in the GW170817 event. In addition several constraints have been imposed to the EOS as, for instance, causality, thermodynamic stability of the star, same EOS for both components of the binary system, and consistency with a maximum mass $M_{\max}/M_\odot = 1.97$. For the calculations in this work the pressure in the NL3e model exceeds the upper limit by a small 3% when hyperons are present and by more than 7% in the NH case. The remaining models do not present hyperons at such density, and the pressure is greater than the reference value 3.5 dyn/cm^2, by 20% in the M$\sigma\delta$ and by 40% in the GM1e case. Notwithstanding, the predicted values are consistent with the experimental bounds.

The different sets of equations of state are used in the following to study the structure of a nonrotating neutron star, for a reasonable range of central pressures. The relation $M(R)$ is shown in Fig. 2 for all the models considered here. An immediate conclusion is that the use of the BM always gives smaller masses, and the predicted maximum mass is far from the empirical bound

TABLE I. The threshold density for the deconfinement transition, the isolated neutron star properties maximum mass, and its corresponding radius for all the models considered. In the two last columns the radius and the tidal deformability of a star with the canonical mass $M/M_\odot = 1.4$ for selected cases.

Model	n_d/n_0	$M_{\max}/M_\odot$	R (km)	$R_{1.4}$ (km)	$\Lambda_{1.4}$
GM1e NH Bag	2.36	1.79	12.8	⋯	⋯
GM1e Bag	2.40	1.76	12.7	⋯	⋯
GM1e NH NJL	2.55	1.98	13.0	13.9	910.03
GM1e NJL	2.85	1.92	12.7	13.9	⋯
NL3e NH Bag	1.98	1.91	14.1	⋯	⋯
NL3e Bag	2.04	1.88	14.0	⋯	⋯
NL3e NH NJL	1.98	2.08	14.3	14.8	1284.20
NL3e NJL	3.44	2.02	13.9	14.8	1284.20
M$\sigma\delta$ NH Bag	2.66	1.90	12.5	⋯	⋯
M$\sigma\delta$ Bag	3.29	1.86	12.2	⋯	⋯
M$\sigma\delta$ NH NJL	3.04	2.10	12.5	12.6	527.08
M$\sigma\delta$ NJL	4.02	2.00	12.1	12.6	527.20

$M/M_\odot \simeq 2$. The combination with the NJL, instead, produces admissible results. In such case the NH approach systematically obtains greater maximum mass corresponding to a greater star radius. In Table I the numerical outcomes are summarized. In the following, only the models predicting $M_{\max}/M_\odot \geq 1.98$ are considered. For all the approaches shown in this table the neutron star with the standard $M/M_\odot \simeq 1.4$ mass is totally composed of nucleons. The only exception corresponds to the prediction of the M$\sigma\delta$ model which finds a tiny 3% of Λ hyperons in the core of the star. In contrast, the central region of the star with maximum mass is in the coexistence phase. There are strange degrees of freedom present in the form of hyperons or as deconfined quarks. Regarding the star with $M/M_\odot = 1.4$, the results for its radius can be compared with the estimates provided by [27]. Both, GM1e and NL3e predictions are well above the upper bound established in that work. The M$\sigma\delta$, instead, gives $R = 12.6$ km that is compatible with the ranges $12.33^{+0.76}_{-0.81}$ km and $12.18^{+0.56}_{-0.79}$ km obtained by different approaches in [27]. For further comparison one can take the Bayesian analysis presented in [48] for the massive pulsar PSR J0740 + 6620, which obtains the radius $R = 12.39^{+1.30}_{-0.98}$ for the star with $M/M_\odot = 2.072^{+0.067}_{-0.066}$. Focusing on the M$\sigma\delta$ model, it gives a star with maximum mass $M/M_\odot = 2.003$ with a radius $R = 12.097$ km, while the NH case indicates that for a star with $M/M_\odot = 2.07$ corresponds a radius $R = 12.67$ km. Although the mass of the first result is slightly below the interval given by [48], the radius of both instances are well in agreement with the range expected by that work. The reliability of the values obtained with the M$\sigma\delta$ is also confirmed by contrasting with [49]. In that work the information on PSR J0740 + 6620 is extended by including additional empirical data to estimate the range $R = 12.45 \pm 0.65$ km for $M/M_\odot = 1.4$ and $R = 12.35 \pm 0.75$ km for the PSR J0740 + 6620.

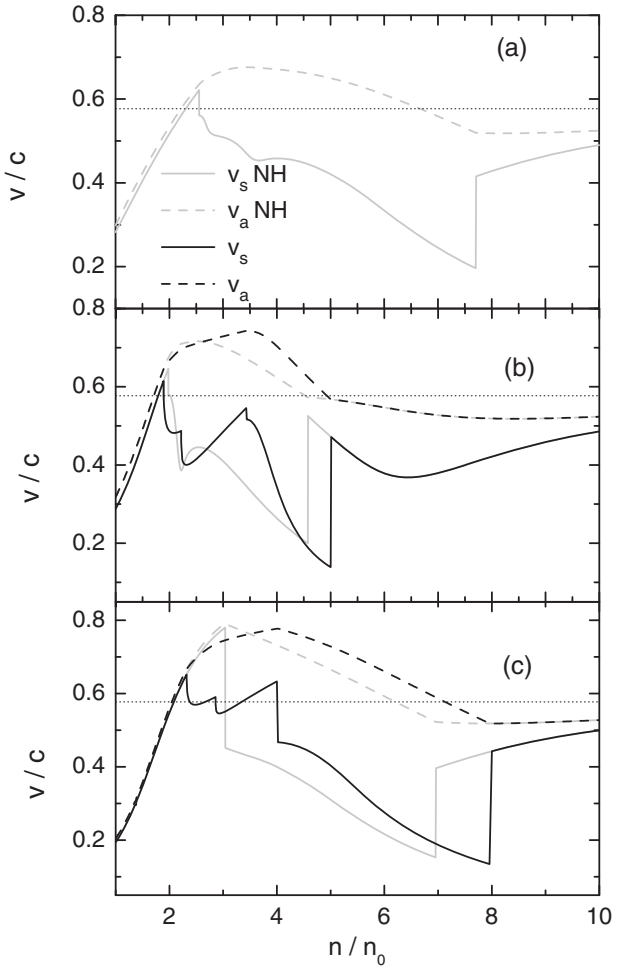

FIG. 3. The speed of sound as a function of the baryonic density for the hadronic models GM1e (a), NL3e (b), and M$\sigma\delta$ (c). The different definitions, equilibrium v_s and adiabatic v_a, corresponding to the cases with or without hyperons (NH) have been distinguished according to the line convention shown. The conformal limit is represented by a horizontal dotted line.

In Fig. 3 the rich structure of the speed of sound for the five models selected is shown in terms of the baryonic density. The panel (a), corresponding to the GM1e NH in combination with the NJL, makes evident some common features; v_a is continuous but v_s presents finite discontinuities at the borders of the coexistence domain, as it has already been noted in [39]. Furthermore, both definitions are almost coincident for low densities and seems to converge to a common value for extremely large densities. In the regime of pure quark matter the variation of v_s is around 6% of the speed of light for the range of densities shown in that figure. In the center of the maximum mass star, corresponding to $n/n_0 \simeq 4.9$, a change $\Delta\mathcal{E} \simeq 1$ fm^{-4} causes a drop in v_s of around 8% the speed of light. The panels (b) and (c) additionally incorporate the effect of hyperons. In such case the general trend of v_a is not highly

modified, but v_s reflects markedly the onset of the hyperons that happens before the deconfinement transition. The Λ baryon appears at $n/n_0 = 1.9(2.3)$, while the heavier Ξ^- starts at $n/n_0 = 2.2(2.8)$ in the NL3e (M$\sigma\delta$) model. The corresponding curve shows a peak followed by a pronounced drop associated with the jumping-off point of each hyperon. The same kind of structure has been observed in [37] at the rise of the hyperon population, using a model of composite baryons, which does not take account of the deconfinement process. Significatively, the peak values are almost coincident, $v_{\max}/c = 0.63$, 0.61 and 0.65 in [37], for the NL3e and M$\sigma\delta$ models, respectively. Beyond these characteristic configurations, the speed of sound increases until the beginning of the phase transition, where a new drop takes place through a discontinuous jump. The sudden decrease after these peaks induces a noticeable splitting of v_a and v_s. A comparison with the conformal limit, $v_{\lim} = c/\sqrt{3}$, shows that it is exceeded at the onset of the coexistence of phases in the models GM1e NH and M$\sigma\delta$ case. In the latter case the difference becomes noticeable in the NH approach, where the increment $\Delta v_s \simeq v_{\lim}/3$ is reached at the threshold density n_t. When hyperons are included in the same framework, n_t is shifted to higher values, and the relative difference is considerably reduced. However, additional points appear where $v_s > v_{\lim}$, corresponding to the onset of the Λ and Ξ^- hyperons. In the first case the excess is as important as in the deconfinement point. The maximum values of v_s obtained in our calculations and discussed in the preceding paragraph must be completed with the cases GM1e NH, NL3e NH, and M$\sigma\delta$ NH giving $v_{\max}/c = 0.62$, 0.64, 0.78, respectively. It must be pointed out that both instances of the M$\sigma\delta$ calculations verify $v_{\max}/c \geq 0.63$, a value that has been proposed as a minimum upper bound for the speed of sound [50]. These observations seem to corroborate the relation between the magnitude of the speed of sound and the number N of effective degrees of freedom. In agreement with the general belief, an increase of N with the density is locally reflected by a sudden drop in v_s, which is realized through a finite discontinuity in the case of the phase transition. The growth of v_s observed between these particular points is consistent with the monotonously increasing trend found in [29], where a variety of nuclear matter equations of state are analyzed. The difference $\tau = 1/c_s^2 - 1/c_a^2$ directly affects the frequency of the nonradial oscillations of a compact star known as gravity modes [39]. For this reason Fig. 4 is devoted to show τ as a function of the baryonic density for the M$\sigma\delta$ model including, or not, the hyperons. In the upper panel a detail of the numerator $c_a^2 - c_s^2$ is presented, where the case NH is suitable for comparison with Fig. 6 of [39]. The monotonous decrease in the coexistence zone and the higher values corresponding to the low density threshold in the present calculations contrast with the results shown in that figure. The inclusion of hyperons has the notorious effect of a sudden rise preceding the discontinuity at n_t.

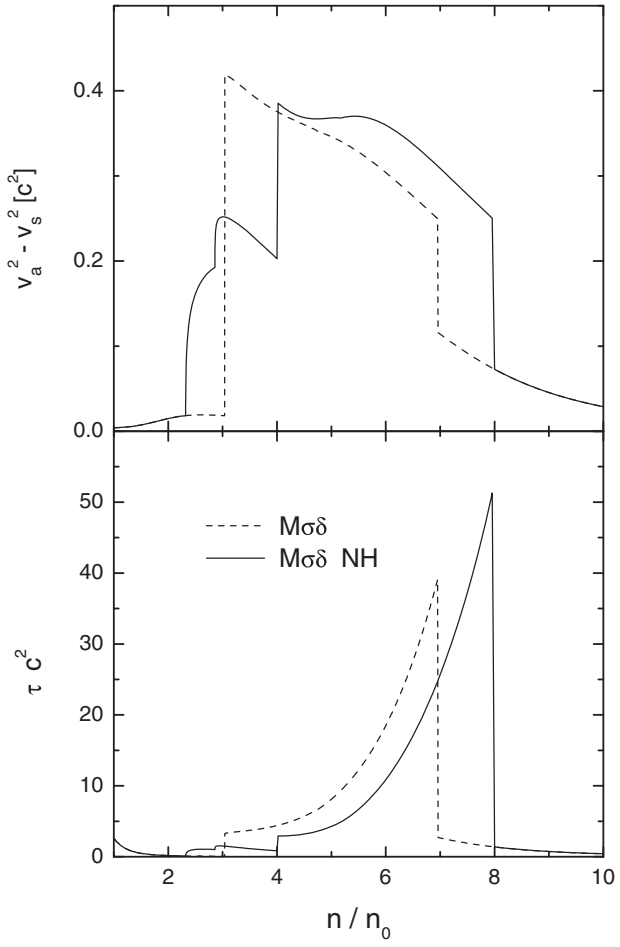

FIG. 4. The combinations of the different definitions of the speed of sound $v_a^2 - v_s^2$ (upper panel) and $\tau = 1/v_s^2 - 1/v_a^2$ (lower panel) as functions of the baryonic density. The cases with or without hyperons (NH) have been distinguished according to the line convention shown.

In the lower panel the full factor τ is presented. The discontinuities, and a preceding staircase structure in the full hyperon treatment, stand out for medium densities. They are diminished by the strong drop experienced at the end of the coexistence region. However, this regime would not be reached since according to the present calculations the pure quark phase state is not realized even for the most massive neutron star.

As a final item, I analyze the predictions for the tidal deformability on the members of a binary system. Taking as a reference a neutron star with $M/M_\odot = 1.4$, the results obtained for the tidal deformability are shown in the last column of Table I. Both GM1e and NL3e results are far beyond the bound, $\Lambda_{1.4} = 190^{+390}_{-120}$, suggested in [6]. The results of both instances of the M$\sigma\delta$, instead, are admissible according to the same criterium but are close to the upper limit. For all the cases considered the central density n_c of the reference star is relatively small, $1.9 \leq n/n_0 \leq 2.5$, and the conventional degrees of freedom of nuclear physics

are the main ingredients of this low mass star. Therefore, the result for $\Lambda_{1.4}$ is intrinsic to the parametrization of the models since the range of densities are reasonably close to the reference point $n/n_0 = 1$. It is surprising that the model inspired in the NL3 parametrization, which accurately describes the structure of several atomic nuclei, has the worst disagreement with the empirical expectations. Another parameter of interest is the combined tidal deformability

$$\tilde{\Lambda} = \frac{16}{13}\frac{\Lambda_1(M_1 + 12M_2)M_1^4 + \Lambda_2(M_2 + 12M_1)M_2^4}{(M_1 + M_2)^5},$$

where M_i, Λ_i are the mass and the tidal deformability of the individual components. On the other hand the chirp mass, given by the relation

$$\mathcal{M}^5 = \frac{M_1^3 M_2^3}{M_1 + M_2},$$

has been determined with accuracy [6] for the event GW170817, while the possible values for M_1 are expected to range within $1.3 < M_1/M_\odot < 1.6$, assuming $M_2 < M_1$. Under this constraint I have evaluated $\tilde{\Lambda}$ in terms of M_1 for the combined M$\sigma\delta$ and NJL models. The result, as shown in Fig. 5, lies between $566 < \tilde{\Lambda} < 608$, which is compatible with the expectations for the low spin prior $\tilde{\Lambda} \in (70, 800)$ as well for the high spin prior $\tilde{\Lambda} \in (0, 630)$ [51]. In the present calculations a coexisting phase of confined and unbound quarks is assumed, which can be interpreted as a consequence of a vanishing interface tension σ_T. At the opposite extreme, for very large σ_T, a discontinuous transition takes place according to the Maxwell construction. For intermediate values a nonhomogeneous phase is expected, which can affect the neutron star properties. These effects have been analyzed in [52] within a specific model, concluding that all of them, the maximum mass, the radius, and the combined tidal deformability monotonously increase with σ_T. An estimation of the maximum variation due to finite tension is given there as $\Delta M_{\max}/M_\odot = 0.02, \Delta R = 0.6$ km, and $\Delta\tilde{\Lambda}/\tilde{\Lambda} = 0.5$ [52]. Thus a scarce increase in the maximum mass can be obtained at the cost of a small growth of the radius and a considerable increment of the tidal deformability.

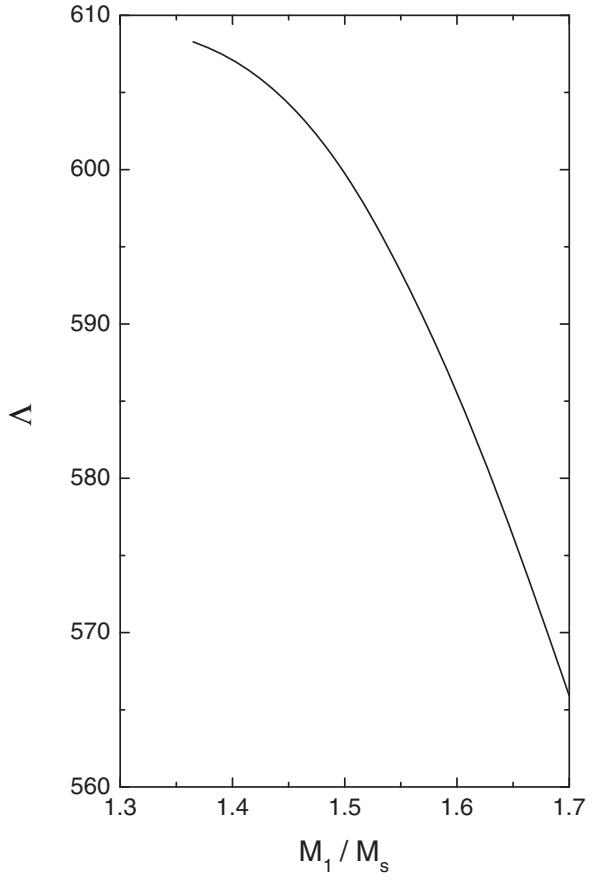

FIG. 5. The combined tidal deformability as a function of the mass of the heavier component of a binary system for the M$\sigma\delta$ model.

The present calculations indicate that the properties of the standard $M/M_\odot = 1.4$ star are determined exclusively by the hadronic EOS, while the deconfined quark EOS could affect the structure of the more massive stars. Therefore, the effect of new configurations in the deconfined phase, such as superconductivity, are of interest for determining the upper limit of the neutron star masses. A large number of studies have focused the effects of superconducting quark matter on the properties of compact stars [53–57]. For instance, in [53] an effective nuclear model is used in combination with a BM, including a color-flavor locked superconducting phase. For the latter model the parameters are taken as $B = 137$ MeV/fm^3, $m_s = 200$ MeV, and $\Delta = 100$ MeV for the energy gap. The mass-radius relation for the neutron star shows the significant fact that a sharp quark-hadron phase transition leads to an unstable star structure. In contrast, the continuous phase transition allows the existence of stable configurations with unbound quarks. In any case the maximum mass is slightly reduced as compared with the unpaired case. This behavior is qualitatively confirmed in [54], where the dynamics of the deconfined quarks are determined by the NJL within two different parametrizations. Since the quark-quark interaction is unknown, the authors assume the same coupling constant as in the four fields quark-antiquark interaction $G_D = G$. They only consider a sharp hadron-quark phase transition and also include the possibility of a light quark superconducting phase (2SC), with unpaired strange flavor, in addition to the just mentioned color-flavor locked arrangement. In this case, the presence of the intermediate two-flavor pairing introduces a narrow window of stability before the color-flavor locked phase becomes preferable. These types of instabilities have been related to the lack of confinement of the NJL model [58] and attributed to the value of the constant $\mathcal{E}_0$, see Eq. (3), used to render zero the energy density at zero baryonic density.

This argument has been examined in [56], where a different procedure to fix the additive constant has been proposed. With this modified constant $\mathcal{E}_0^*$, an intermediate stable 2SC phase was found, as in [54]. A further increase of the pairing coupling constant to $G_D = 1.2G$, in combination with $\mathcal{E}_0^*$, extends the range of stability to embrace the color-flavor locked phase. At the same time the allowed maximum mass for neutron stars is reduced [56]. Based on these results one can conclude that the inclusion of a superconducting quark phase, if stable, will lead to a decrease of $M_{\max}$.

V. SUMMARY AND CONCLUSIONS

This work is devoted to the study of dense matter at zero temperature, as can be found in the interior of neutron stars. To describe the low and medium densities regime, three models of the field theory of hadrons are used. They have different motivations, while GM1 and the recent M$\sigma\delta$ focus on bulk properties of homogeneous matter, the NL3 was calibrated to study atomic nuclei. In all the cases the formulation has been extended to include hyperons. For high densities a scheme of deconfined quarks are considered using either the bag or the NJL models. In the first case the quarks do not interact, and vacuum effects are explicitly included through the bag constant B, while in the well-known NJL there is a strong interaction between quarks, which give them their constituent masses. In between a coexistence of phases is assumed, which allows a continuous variation of the thermodynamic potential. As an alternative the situation (NH) with hyperons artificially suppressed is also taken into account. In this context the equation of state has been analyzed and the speed of sound, in particular. The effects on the structure of a neutron star have been emphasized, and the contrast with recent observational data has been done. For all the cases considered the hyperons emerge near $n/n_0 = 2$, and the deconfinement transition starts at a higher density n_d, which depends on the model used (see Table I). The well-known fact that the NH approach gives the harder EOS has been corroborated for each model. Furthermore, the combination with the BM systematically gives a softer EOS as compared with the NJL case. The adiabatic speed of sound v_a shows a continuous behavior, while the equilibrium velocity v_s presents finite discontinuities at the extreme points of the coexistence region [39]. I have found that the onset of the hyperons also has noticeable effects, giving place to characteristic breaks of the monotonous variation of v_s. The quantity $1/v_s^2 - 1/v_a^2$, which enters in the construction of the frequency of g-mode oscillations of a star, also has distinctive behaviors according to the presence, or not, of the hyperons. The relation mass radius of an isolated neutron star has been examined and I find that the combinations with the BM are not able to satisfy the requisite $M_{\max}/M_\odot > 1.95$, hence these instances are discarded. Focusing on a star with the canonical mass $M/M_\odot = 1.4$, it is found that its central density is small enough such that only nucleons and leptons are present in its composition. The exception is the M$\sigma\delta$, which predicts a scarce amount of Λ hyperons. When considered as a part of a binary system, its tidal deformability is expected to be bounded by $\Lambda_{1/4} < 580$ [6], however, only the prediction of the M$\sigma\delta$ model, $\Lambda_{1/4} = 527$, adjust this condition. Furthermore, when the experimental value for the chirp mass $\mathcal{M}/M_\odot = 1.186$ is taken into account, the composed tidal deformability has been found to satisfy $566 < \tilde{\Lambda} < 608$, which is compatible with the observational evidence [51]. One can conclude that the formulation of a hadronic model, which includes the hyperons and the realization of a coexistence phase with deconfined quarks, is absolutely compatible with the recent experimental data on compact stars. In the case analyzed in this work, the model denoted as M$\sigma\delta$ [44,45], achieves this purpose with simplicity by introducing only one additional term to those commonly used in the field theory of hadrons. This term consists of a nonlinear meson vertex with a constant coupling and continues the long-standing strategy of representing high density effects by this type of interaction [59]. There are still several open questions about this model which deserve investigation, as for instance, the combination of the δ and the hidden strangeness $f_0(980)$ mesons as mediators of the hyperon interaction, or the compatibility with the phenomenology of atomic nuclei.

ACKNOWLEDGMENTS

This work was partially supported by the CONICET, Argentina under Grant PIP-616.

APPENDIX: MASS DERIVATIVES IN THE NJL MODEL

The derivatives of the constituent quark masses in the NJL are given by

$$M_i' = -4Gn_{si}' + 2K(n_{sj}n_{sk})', \text{ where } i \neq j, \quad i \neq k, \quad j \neq k.$$

In turn the derivatives of the quark condensates are the solutions of a linear set of algebraic equations,

$$\sum_j \mathcal{A}_{ij} n_{sj}' = \frac{p_i}{D}\frac{M_i}{\mu_i}\mathcal{N}_i, \qquad i = u, d, s,$$

where $D = a_u(p_d + p_s) - (a_d + a_s)p_u$, $\mathcal{N}_u = -(a_d + a_s)\pi^2$, $\mathcal{N}_d = \mathcal{N}_s = a_u\pi^2$,

$$a_u = \frac{1}{\mu_u} + \frac{2p_u}{\mu_e \sum_l p_l}, \qquad a_d = -\frac{1}{\mu_d} - \frac{p_d}{\mu_e \sum_l p_l}, \qquad a_s = -\frac{p_s}{\mu_e \sum_l p_l},$$

and

$$\mathcal{A}_{ij} = \left(\frac{\pi^2}{3} - 4GF_i\right)\delta_{ij} + 2KF_i n_{sm}(1-\delta_{ij}) + 2\frac{p_i}{D}\frac{M_i}{\mu_i}\left(2G\mathcal{P}_{ij}\frac{M_j}{\mu_j} - K\sum_{k\neq j} n_{sl}\mathcal{P}_{ik}\frac{M_k}{\mu_k}\right),$$

where $j \neq m \neq i$ and $k \neq l \neq i$, and

$$\mathcal{P} = \begin{pmatrix} -p_d - p_s & p_d & p_s \\ p_u & -p_u + (a_u p_s - a_s p_u)\mu_d & (a_u p_s - a_s p_u)\mu_d \\ p_u & -p_u + (a_u p_d - a_d p_u)\mu_d & (a_d p_u - a_u p_d)\mu_d \end{pmatrix}.$$

[1] P. B. Demorest, T. Pennucci, S. M. Ransom, M. S. E. Roberts, and J. W. T. Hessels, Nature (London) **467**, 1081 (2010).
[2] R. W. Romani, D. Kandel, A. V. Filippenko, T. G. Brink, and W. Zheng, Astrophys. J. Lett. **908**, L46 (2021).
[3] E. Fonseca *et al.*, Astrophys. J. Lett. **915**, L12 (2021).
[4] T. Hinderer, Astrophys. J. **677**, 1216 (2008).
[5] B. P. Abbott *et al.*, Phys. Rev. Lett. **119**, 161101 (2017).
[6] B. P. Abbott *et al.*, Phys. Rev. Lett. **121**, 161101 (2018).
[7] K. Takami, L. Rezzolla, and L. Baiotti, Phys. Rev. Lett. **113**, 091104 (2014).
[8] E. R. Most, L. R. Weih, L. Rezzolla, and J. Schaffner-Bielich, Phys. Rev. Lett. **120**, 261103 (2018).
[9] R. Nandi, P. Char, and S. Pal, Phys. Rev. C **99**, 052802(R) (2019).
[10] O. Lourenco, M. Dutra, C. H. Lenzi, C. V. Flores, and D. P. Menezes, Phys. Rev. C **99**, 045202 (2019).
[11] J. J. Li and A. Sedrakian, Astrophys. J. Lett. **874**, L22 (2019).
[12] S. Traversi, P. Char, and G. Pagliara, Astrophys. J. **897**, 165 (2020).
[13] R. O. Gomes, P. Char, and S. Schramm, Astrophys. J. **877**, 139 (2019).
[14] S. Han, M. A. A. Mamun, S. Lalit, C. Constantinou, and M. Prakash, Phys. Rev. D **100**, 103022 (2019).
[15] V. Dexheimer, R. O. Gomes, S. Schramm, and H. Pais, J. Phys. G **46**, 034002 (2019).
[16] P. Landry, R. Essick, and K. Chatziioannou, Phys. Rev. D **101**, 123007 (2020).
[17] R. Essick, P. Landry, and D. E. Holz, Phys. Rev. D **101**, 063007 (2020).
[18] R. Essick, I. Tews, P. Landry, S. Reddy, and D. E. Holz, Phys. Rev. C **102**, 055803 (2020); R. Essick, I. Tews, P. Landry, and A. Schwenk, Phys. Rev. Lett. **127**, 192701 (2021); R. Essick, P. Landry, A. Schwenk, and I. Tews, Phys. Rev. C **104**, 065804 (2021).
[19] B. T. Reed, F. J. Fattoyev, C. J. Horowitz, and J. Piekarewicz, Phys. Rev. Lett. **126**, 172503 (2021).
[20] S. Blacker, N. U. F. Bastian, A. Bauswein, D. B. Blaschke, T. Fischer, M. Oertel, T. Soultanis, and S. Typel, Phys. Rev. D **102**, 123023 (2020).
[21] S. Y. Lau and K. Yagi, Phys. Rev. D **103**, 063015 (2021).
[22] I. Legred, K. Chatziioannou, R. Essick, S. Han, and P. Landry, Phys. Rev. D **104**, 063003 (2021).
[23] P. T. H. Pang, I. Tews, M. W. Coughlin, M. Bulla, C. Van Den Broeck, and T. Dietrich, Astrophys. J. **922**, 14 (2021).
[24] E. R. Most, L. J. Papenfort, V. Dexheimer, M. Hanauske, S. Schramm, H. Stocker, and L. Rezzolla, Phys. Rev. Lett. **122**, 061101 (2019); E. R. Most, L. J. Papenfort, V. Dexheimer, M. Hanauske, H. Stocker, and M. Rezzolla, Eur. Phys. J. A **56**, 59 (2020).
[25] M. Ferreira and C. Providencia, Phys. Rev. D **104**, 063006 (2021).
[26] W. Z. Shangguan, Z. Q. Huang, S. N. Wei, and W. Z. Jiang, Phys. Rev. D **104**, 063035 (2021).
[27] G. Raiijmakers, S. K. Greif, K. Hebeler, T. Hinderer, S. Nissanke, A. Schwenk, T. E. Riley, A. L. Watts, J. M. Lattimer, and W. C. G. Ho, Astrophys. J. Lett. **918**, L29 (2021).
[28] P. Bedaque and A. W. Steiner, Phys. Rev. Lett. **114**, 031103 (2015).
[29] Ch. C. Moustakidis, T. Gaitanos, Ch. Margaritis, and G. A. Lalazissis, Phys. Rev. C **95**, 045801 (2017).
[30] E. D. Van Oeveren and J. L. Friedman, Phys. Rev. D **95**, 083014 (2017).
[31] I. Tews, J. Carlson, S. Gandolfi, and S. Reddy, Astrophys. J. **860**, 149 (2018).
[32] N. Zhang, D. Wen, and H. Chen, Phys. Rev. C **99**, 035803 (2019).
[33] B. Reed and C. J. Horowitz, Phys. Rev. C **101**, 045803 (2020).
[34] Ch. Margaritis, P. S. Koliogiannis, and Ch. C. Moustakidis, Phys. Rev. D **101**, 043023 (2020).
[35] A. Kanakis-Pegios, P. S. Koliogiannis, and Ch. C. Moustakidis, Phys. Rev. C **102**, 055801 (2020).

[36] M. G. Alford, S. Han, and M. Prakash, Phys. Rev. D **88**, 083013 (2013).
[37] T. F. Motta, P. A. M. Guichon, and A. W. Thomas, Nucl. Phys. **A1009**, 122157 (2021).
[38] H. Tan, T. Dore, V. Dexheimer, J. Noronha-Hostler, and N. Yunes, Phys. Rev. D **105**, 023018 (2022).
[39] P. Jaikumar, A. Semposki, M. Prakash, and C. Constantinou, Phys. Rev. D **103**, 123009 (2021).
[40] N. K. Glendenning and S. A. Moszkowski, Phys. Rev. Lett. **67**, 2414 (1991).
[41] S. Weissenborn, D. Chatterjee, and J. Schaffner Bielich, Nucl. Phys. **A881**, 62 (2012).
[42] G. A. Lalazissis, J. Konig, and P. Ring, Phys. Rev. C **55**, 540 (1997).
[43] F. Yang and H. Shen, Phys. Rev. C **77**, 025801 (2008).
[44] S. Kubis, W. Wojcik, and N. Zabari, Phys. Rev. C **102**, 065803 (2020).
[45] T. Miyatsu, M.-K. Cheoun, and K. Saito, Astrophys. J. **929**, 82 (2022).
[46] G. Baym, C. Pethick, and P. Sutherland, Astrophys. J. **170**, 299 (1971).
[47] T. Hatsuda and T. Kunihiro, Phys. Rep. **247**, 221 (1994).
[48] T. E. Riley *et al.*, Astrophys. J. Lett. **918**, L27 (2021).
[49] M. C. Miller *et al.*, Astrophys. J. Lett. **918**, L28 (2021).
[50] J. Alsing, H. O. Silva, and E. Berti, Mon. Not. R. Astron. Soc. **478**, 1377 (2018).
[51] B. P. Abbott *et al.*, Phys. Rev. X **9**, 011001 (2019).
[52] C. J. Xia, T. Maruyama, N. Yasutake, and T. Tatsumi, Phys. Rev. D **99**, 103017 (2019).
[53] M. Alford and S. Reddy, Phys. Rev. D **67**, 074024 (2003).
[54] M. Buballa, F. Neumann, M. Oertel, and I. Shovkovy, Phys. Lett. B **595**, 36 (2004).
[55] S. Lawley, W. Bentz, and A. W. Thomas, J. Phys. G **32**, 667 (2006).
[56] G. Pagliara and J. Schaffner-Bielich, Phys. Rev. D **77**, 063004 (2008).
[57] I. Paulucci, E. J. Ferrer, J. E. Horvath, and V. de la Incera, J. Phys. G **40**, 125202 (2013).
[58] M. Baldo, G. F. Burgio, P. Castorina, S. Plumari, and D. Zappala, Phys. Rev. C **75**, 035804 (2007).
[59] J. Boguta and A. R. Bodmer, Nucl. Phys. **A292**, 413 (1977).